Chemical Engineering Journal 93 (2003) 191–200

Chemical Engineering Journal

www.elsevier.com/locate/cej

# Study on the alkylation of benzene and 1-dodecene

Zhigang Lei, Chengyue Li*, Biaohua Chen, Wang Erqiang, Jinchang Zhang

*The Key Laboratory of Science and Technology of Controllable Chemical Reactions, Ministry of Education, Beijing University of Chemical Technology, P.O. Box 35, Beijing 100029, China*

Received 22 May 2002; accepted 26 October 2002

**Abstract**

Linear alkylation (LAB) is an important intermediate in the detergent industry. This work deals with the suspension catalytic distillation (SCD) column used for synthesis of C12 alkylbenzene with benzene and 1-dodecene. A novel solid catalyst, which is friendly to environment, was selected. The kinetic equations using this catalyst were measured in a fixed-bed reactor. The mathematical models of equilibrium (EQ) stage and nonequilibrium (NEQ) stage for alkylation of benzene and 1-dodecene were, respectively, established by incorporating the kinetic equations to simulate the SCD column. By comparison of the results from experiments, it was concluded that the NEQ stage model was more accurate than the EQ stage model for the simulation.


*Keywords:* Suspension catalytic distillation (SCD); Equilibrium (EQ) stage model; Nonequilibrium (NEQ) stage model; Benzene; 1-Dodecene; Alkylation

## 1. Introduction

Linear alkylation (LAB) is an important intermediate in the detergent industry, and is usually made from alkylation of benzene and olefin with long carbon chains from C10 to C14. The catalysts for alkylation reaction are generally aluminium trichloride ($AlCl_3$), hydrofluoric acid (HF) and solid acids. But it is known that $AlCl_3$ and HF are, to some extents, hazardous to environment. Many efforts have been made to replace it with environmentally safer solid catalysts such as H-ZSM-5, H-ZSM-12, HY and lays [1,2].

However, the common solid catalysts have the drawbacks, that is, low conversion, low selectivity and high ratio of benzene and olefin. In order to overcome those, a high-efficient heteropoly acid catalyst which is friendly to environment is developed [3]. The catalyst used in this work is made up of 77 wt.% silica gel and 28 wt.% tungstophosphoric acid (HPW), and of high activity and selectivity for alkylation of benzene and 1-dodecene. But formerly the kinetics equations for the reaction over any catalyst were rarely reported in open references.

With the development of chemical engineering, the process of distillation coupled with reaction, namely reactive distillation (RD), has been devised for many years. RD has been applied in the industry, e.g. the manufactures of methyl acetate and methyl *tert*-butyl ether [4–7]. In general, RD is divided into two categories: homogeneous and heterogeneous catalytic distillation. Moreover, heterogeneous catalytic distillation is a more recent development and has attracted researchers' attention because the difficulty in separation between products and catalysts is easy to be overcome. In recent years, a new-type heterogeneous catalytic distillation column, called suspension catalytic distillation (SCD) column, has been put forward by Wen et al. [8]. But the work on the SCD column is very scarce. In the SCD column, tiny solid particles are not used as packing in the column but blended with liquid phase. Compared to conventional RD column, it has the following unique advantages: (1) no need for structured catalytic-packing; (2) no need for shutting down the unit to replace the deactivated catalyst; (3) mass and heat transfers in the fine catalyst particles and interphase are quicker than those in the structured catalytic-packing. However, it is believed that the packed column is not suitable for the SCD column. When adding solid particles to liquid phase, the packed column is prone to be jammed. From this viewpoint, the tray column is more suitable for the SCD column.

In this work, the SCD column is used for synthesis of C12 alkylbenzene with benzene and 1-dodecene. Firstly, the kinetics equations over the heteropoly acid catalyst are measured in a fixed-bed micro-reactor. Then, the mathematical models of the SCD column are established by incorporating the kinetic equations. To date there are two types of mathematical models to simulate reactive or nonreactive

* Corresponding author. Tel.: +8610-64433695; fax: +8610-644336787.
*E-mail address:* licy@mail.buct.edu.cn (C. Li).

1385-8947/02/$ – see front matter 
PII: S1385-8947(02)00318-2

**Nomenclature**

| | |
|---|---|
| $c$ | number of components |
| $c_t$ | total concentration (kmol m$^{-3}$) |
| $C$ | mole concentration in the liquid phase (kmol m$^{-3}$) |
| $D_{i,k}$ | Maxwell–Stefan diffusivity (m$^2$ s$^{-1}$) |
| $E$ | energy transfer rate (kJ s$^{-1}$) |
| $F$ | feed flowrate (kmol h$^{-1}$) |
| $h$ | heat transfer coefficient (W (m$^2$ K)$^{-1}$) |
| $H$ | molar enthalpy (kJ kmol$^{-1}$) |
| $K$ | vapor–liquid equilibrium constant |
| $L$ | liquid flowrate (kmol h$^{-1}$) |
| $M$ | hold-up in the stage (kmol) |
| $N$ | mass transfer rate (kmol h$^{-1}$) |
| $P$ | stage pressure (kPa) |
| $Q$ | heat duty (kJ h$^{-1}$) |
| $r$ | number of reactions |
| $r_{i\text{-ph}}$ | reaction rate (kmol (kg s)$^{-1}$) |
| $r_j$ | ratio of sidestream flowrate to interstage flowrate |
| $R$ | gas constant (kJ (kmol K)$^{-1}$) |
| $R_{k,j}$ | reaction rate (kmol (kg s)$^{-1}$) |
| $S$ | flowrate of the sidestream (kmol h$^{-1}$) |
| $t$ | time (h) |
| $T$ | Temperature (K) |
| $v$ | stoichiometric coefficient |
| $V$ | vapor flowrate (kmol h$^{-1}$) |
| $x$ | mole fraction in the liquid phase |
| $y$ | mole fraction in the vapor phase |
| $z$ | mole fraction in the feed |

*Greek symbols*

| | |
|---|---|
| $\gamma$ | activity coefficient |
| $\varepsilon$ | catalyst weight (kg) |
| $\eta$ | dimensionless coordinate |
| $\kappa$ | mass transfer coefficient (m s$^{-1}$) |
| $\mu$ | chemical potential (kJ kmol$^{-1}$) |

*Subscripts*

| | |
|---|---|
| 0 | referring to saturated condition |
| 1, 2, 3, 4, 5 | reaction index |
| $i$, $k$ | component number |
| I | referring to interface |
| $j$ | stage number |

*Superscripts*

| | |
|---|---|
| cal | calculated value |
| exp | experimental value |
| F | referring to feed stream |
| L | referring to liquid phase |
| LF | referring to liquid diffusion film |
| V | referring to vapor phase |
| VF | referring to vapor diffusion film |

distillation systems, e.g. the equilibrium (EQ) and nonequilibrium (NEQ) stage models. In this work, these two models are, respectively, programmed to simulate the SCD column, and the results are compared with those from experiments.

## 2. Kinetic equations

In general, the kinetic property of a chemical reaction that is carried out in a distillation column should be measured separately, e.g. in a fixed-bed reactor. Moreover, in case of heterogeneous catalytic reaction, special attention should be paid to the mass and energy transport resistance inside the catalyst. Thus, both micro- and macro-kinetics of the reaction system must be studied carefully. Herein, it is assumed that intrinsic reaction rates are the same as global rates because the catalyst used in the SCD column is tiny particles and situated in strong turbulence so that the mass and energy transport resistances inside and outside the catalyst particles can be neglected.

The involved reaction network for alkylation of benzene and 1-dodecene is expressed as [9]

$$\mathrm{B} + \mathrm{D} \xrightarrow{k_1} \text{2-ph}$$

$$\mathrm{B} + \mathrm{D} \xrightarrow{k_2} \text{3-ph}$$

$$\mathrm{B} + \mathrm{D} \xrightarrow{k_3} \text{4-ph}$$

$$\mathrm{B} + \mathrm{D} \xrightarrow{k_4} \text{5-ph}$$

$$\mathrm{B} + \mathrm{D} \xrightarrow{k_5} \text{6-ph}$$

where B, D, and $i$-ph ($i = 2$–6) represent benzene, 1-dodecene and five different positional alkylbenzene (phenyldodecane isomers), respectively. It is possible that some heavier byproducts, such as multi-alkylbenzene, also form. But it is apparent that those are too small to be neglected.

The kinetic equations for alkylation of benzene and 1-dodecene were determined in a fixed-bed micro-reactor, schematized in Fig. 1. The experimental system comprised of three parts, a feed blending station for preparing the reaction mixture with different composition, an assembly of electric oven with a multi-channel temperature controller, and an off-line gas chromatogram (GC) and gas chromatogram-mass spectrometer (GC-MS).

The feed blending station consisted of two metering pumps for driving benzene and 1-dodecene, respectively, a nitrogen tube for sweeping and a mixer. The metering pumps were calibrated in advance. Feed composition was calculated based on the reading of the metering pumps and checked by gas chromatogram analysis.

The main parts of electric oven assembly are a fixed-bed micro-reactor of 8 mm i.d., 300 mm long, and an heating-oven of 800 W. The temperature of reaction section was controlled with a temperature programmable controller

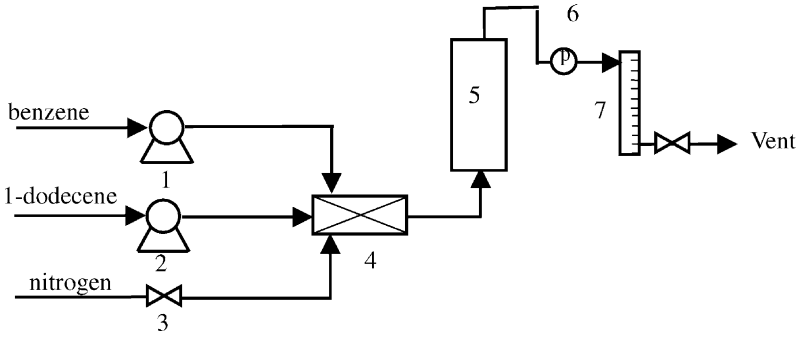


Fig. 1. The schematic diagram of fixed-bed micro-reactor: (1) benzene metering pump; (2) 1-dodecene metering pump; (3) adjusting valve; (4) mixer; (5) fixed-bed micro-reactor; (6) pressure adjusting valve; (7) metering vessel.

and measured with a micro-thermal couple inserted in its center through a small jacket tube. The reaction section of the reactor was charged with 0.2 g catalyst and some amount of quartz chips was loaded in both sides of the reaction section. Suitable particle size of the catalyst was determined by a preliminary experiment so as to eliminate the influence of internal diffusion. A back-pressure regulator was equipped downstream in the micro-reactor. The composition analysis system for feed and product consisted of an off-line gas chromatogram, SP 3420, equipped with a FID detector and an OV-101 capillary column (60 m long and 0.32 mm o.d.).

The reaction was performed at temperatures between 358.15 and 398.15 K. The series of experiments was arranged according to the principle of mathematical statistics. The pre-experiments were done to investigate the influence of external and internal diffusions. It was found that when the average diameter of catalyst particles was less than 0.21 nm (60–80 mesh) and the liquid weight hourly space velocity (WHSV) was larger than 20 $h^{-1}$, the influence of external and internal diffusions may be thought to preclude.

The kinetic data are listed in Table 1, from which the kinetic equations for alkylation of benzene and 1-dodecene were obtained after correlating by the Marquardt method

Table 1
The kinetic data obtained in the fixed-bed micro-reactor

| Temperature (K) | Mole concentration (kmol $m^{-3}$) | | Reaction rate (kmol $(m^3\,kg)^{-1}$) | | | | |
|---|---|---|---|---|---|---|---|
| | Benzene | 1-Dodecene | 6-Ph | 5-Ph | 4-Ph | 3-Ph | 2-Ph |
| 358.15 | 7.043 | 1.691 | 0.00025 | 0.00115 | 0.00087 | 0.001162 | 0.001282 |
| | 8.451 | 1.127 | 0.00024 | 0.00084 | 0.00069 | 0.001114 | 0.000946 |
| | 9.351 | 0.767 | 0.00017 | 0.00063 | 0.00062 | 0.000839 | 0.000707 |
| | 9.799 | 0.588 | 0.00014 | 0.00051 | 0.00042 | 0.000678 | 0.000547 |
| | 10.044 | 0.490 | 0.00011 | 0.00044 | 0.00037 | 0.000586 | 0.000579 |
| 368.15 | 7.043 | 1.691 | 0.00037 | 0.00156 | 0.00135 | 0.003280 | 0.001865 |
| | 8.451 | 1.127 | 0.00029 | 0.00115 | 0.00114 | 0.002340 | 0.001332 |
| | 9.351 | 0.767 | 0.00024 | 0.00094 | 0.00076 | 0.001780 | 0.000970 |
| | 9.799 | 0.588 | 0.00021 | 0.00066 | 0.00062 | 0.001480 | 0.000806 |
| | 10.044 | 0.490 | 0.00019 | 0.00062 | 0.00051 | 0.001243 | 0.000788 |
| 378.15 | 7.043 | 1.691 | 0.00050 | 0.00227 | 0.00182 | 0.003280 | 0.002010 |
| | 8.451 | 1.127 | 0.00041 | 0.00182 | 0.00162 | 0.002340 | 0.001857 |
| | 9.351 | 0.767 | 0.00035 | 0.00147 | 0.00107 | 0.001780 | 0.001399 |
| | 9.799 | 0.588 | 0.00032 | 0.00125 | 0.00080 | 0.001480 | 0.001120 |
| | 10.044 | 0.490 | 0.00027 | 0.00084 | 0.00076 | 0.001243 | 0.000959 |
| 388.15 | 7.043 | 1.691 | 0.00086 | 0.00324 | 0.00330 | 0.004400 | 0.002982 |
| | 8.451 | 1.127 | 0.00067 | 0.00259 | 0.00274 | 0.003700 | 0.002535 |
| | 9.351 | 0.767 | 0.00058 | 0.00215 | 0.00174 | 0.002380 | 0.002012 |
| | 9.799 | 0.588 | 0.00043 | 0.00137 | 0.00130 | 0.001837 | 0.001547 |
| | 10.044 | 0.490 | 0.00040 | 0.00144 | 0.00111 | 0.001629 | 0.001302 |
| 398.15 | 7.043 | 1.691 | 0.00119 | 0.00464 | 0.00425 | 0.005630 | 0.004082 |
| | 8.451 | 1.127 | 0.00101 | 0.00345 | 0.00310 | 0.004740 | 0.003436 |
| | 9.351 | 0.767 | 0.00084 | 0.00264 | 0.00236 | 0.003440 | 0.002585 |
| | 10.044 | 0.490 | 0.00057 | 0.00168 | 0.00151 | 0.002124 | 0.001796 |

and written as follows:

$$r_{2\text{-ph}} = 402.783 \times \exp\left(-\frac{45,734}{RT}\right) C_B C_D \quad (1)$$

$$r_{3\text{-ph}} = 743.969 \times \exp\left(-\frac{46,649}{RT}\right) C_B C_D \quad (2)$$

$$r_{4\text{-ph}} = 792.109 \times \exp\left(-\frac{48,080}{RT}\right) C_B C_D \quad (3)$$

$$r_{5\text{-ph}} = 892.208 \times \exp\left(-\frac{48,080}{RT}\right) C_B C_D \quad (4)$$

$$r_{6\text{-ph}} = 217.870 \times \exp\left(-\frac{48,225}{RT}\right) C_B C_D \quad (5)$$

where $R$ is gas constant (8.314 kJ (kmol K)$^{-1}$), $T$ the temperature (K), $C$ the mole concentration (kmol m$^{-3}$) in the liquid phase, and $r$ is the reaction rate for specified component (kmol (m$^3$ kg)$^{-1}$ catalyst). The kinetic equations were verified by $F$-factor test, and thought to be reliable because it was consistent with the $F$-factor rules.

## 3. EQ stage and NEQ stage models

For design of reactive distillation, two types of modeling approaches have been developed: the EQ and the NEQ stage models [10–15]. The schematic diagrams of a tray column for each model are shown in Figs. 2 and 3, respectively. The most difference between both the figures is that the mass and heat transfer rates are considered in every tray in the NEQ stage model. The assumptions used in this study for each model are summarized in Table 2.

The equations that model EQ stages are known as the MESHR equations [11]. MESHR is an acronym referring to the different types of equation. The M equations are the material balance equations. The total material balance takes the form

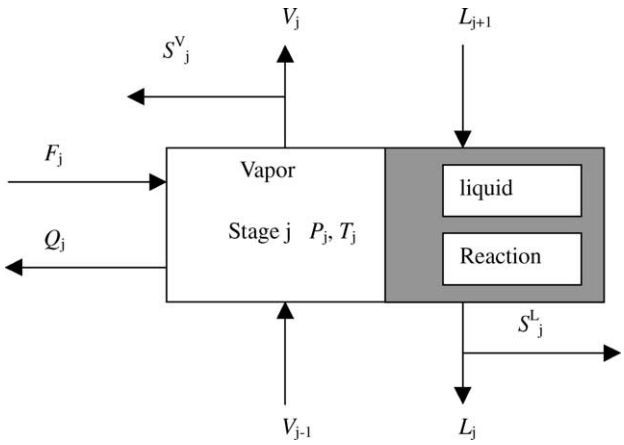


Fig. 2. Schematic representation of an EQ stage.

$$\frac{dM_j}{dt} = V_{j+1} + L_{j-1} + F_j - (1 + r_j^V)V_j - (1 + r_j^L)L_j + \sum_{k=1}^{r}\sum_{i=1}^{c} v_{i,k} R_{k,j} \varepsilon_j \quad (6)$$

$M_j$ is the hold-up on stage $j$. With very few exceptions, $M_j$ is considered to be the hold-up only of the liquid phase. It is more important to include the hold-up of the vapor phase at higher pressures. The component material balance (neglecting the vapor hold-up) is

$$\frac{dM_j x_{i,j}}{dt} = V_{j+1} y_{i,j+1} + L_{j-1} x_{i,j-1} + F_j z_{i,j} - (1 + r_j^V)V_j y_{i,j} - (1 + r_j^L)L_j x_{i,j} + \sum_{k=1}^{r} v_{i,k} R_{k,j} \varepsilon_j \quad (7)$$

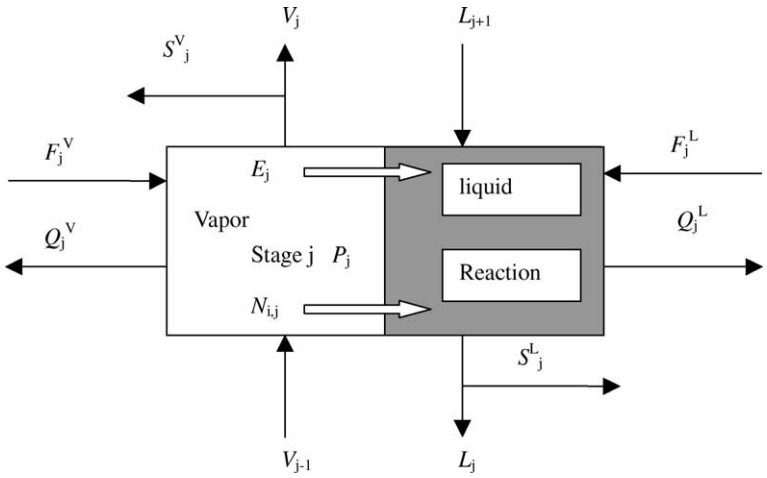


Fig. 3. Schematic representation of an NEQ stage.

Table 2
Assumptions used in the EQ and NEQ stage models

| EQ stage model | NEQ stage model |
|---|---|
| (1) Operation reaches steady state | (1) Operation reaches steady state |
| (2) System reaches mechanical equilibrium | (2) System reaches mechanical equilibrium |
| (3) The vapor and liquid bulks are mixed perfectly and assumed to be at thermodynamic equilibrium | (3) The vapor–liquid interface is uniform in each tray and assumed to be at thermodynamic equilibrium |
| (4) Heat of mixing can be neglected | (4) Heat of mixing can be neglected |
| (5) Reactions take place in the liquid bulk | (5) There is no accumulation of mass and heat at the interface |
| (6) The condenser and reboiler are considered as an equilibrium tray | (6) The condenser and reboiler are considered as an equilibrium tray |
| (7) The amount of catalyst in each tray of reactive section is equal | (7) Reactions within the interface are ignored and take place in the liquid bulk |
| (8) The influence of catalyst on the mass and energy balance is neglected because the catalyst concentration in the liquid phase is low (0.05 g ml$^{-1}$) | (8) The amount of catalyst in each tray of reactive section is equal |
| | (9) The influence of catalyst on the mass and energy balance is neglected because the catalyst concentration in the liquid phase is low (0.05 g ml$^{-1}$) |

In the material balance equations given above, $r_j$ is the ratio of sidestream flow to interstage flow:

$$r_j^{\mathrm{V}} = \frac{S_j^{\mathrm{V}}}{V_j}, \qquad r_j^{\mathrm{L}} = \frac{S_j^{\mathrm{L}}}{L_j} \tag{8}$$

$v_{i,k}$ represents the stoichiometric coefficient of the component $i$ in reaction $k$ and $\varepsilon_j$ represents the amount of catalyst.

The E equations are the phase equilibrium relations:

$$y_{i,j} = K_{i,j} x_{i,j} \tag{9}$$

The S equations are the summation equations:

$$\sum_{i=1}^{c} x_{i,j} = 1, \qquad \sum_{i=1}^{c} y_{i,j} = 1 \tag{10}$$

The enthalpy balance is given by

$$\frac{\mathrm{d}M_j H_j}{\mathrm{d}t} = V_{j+1}H_{j+1}^{\mathrm{V}} + L_{j-1}H_{j-1}^{\mathrm{L}} + F_j H_j^{\mathrm{F}} - (1+r_j^{\mathrm{V}})V_j H_j^{\mathrm{V}} - (1+r_j^{\mathrm{L}})L_j H_j^{\mathrm{L}} - Q_j \tag{11}$$

There is no need to take separate account in Eq. (11) of the heat generated due to chemical reaction since the computed enthalpies include the heats of formation.

The R equations are the reaction rate equations and given in Eqs. (1)–(5).

Under steady-state conditions, all the time derivatives in the MESH equations are equal to zero. The modified relaxation method where the MESH equations are written in unsteady-state form and are integrated numerically until the steady-state solution has been found, is used to solve the above equations [16–19].

The NEQ stage model for reactive distillation follows the philosophy of rate based models for conventional distillation. In the NEQ stage model, it is assumed that the resistance to mass and energy transfer is located in thin film adjacent to the vapor–liquid interface according to the two-film theory [13] (see Fig. 4).

The time rate of change of the number of moles of component $i$ in the vapor ($M_i^{\mathrm{V}}$) and liquid ($M_i^{\mathrm{L}}$) phases on stage $j$ are given by the following balance relations:

$$\frac{\mathrm{d}M_{i,j}^{\mathrm{V}}}{\mathrm{d}t} = V_{j+1}y_{i,j+1} - V_j y_{i,j} + z_{i,j}^{\mathrm{V}}F_{i,j}^{\mathrm{V}} - N_{i,j}^{\mathrm{V}} \tag{12}$$

$$\frac{\mathrm{d}M_{i,j}^{\mathrm{L}}}{\mathrm{d}t} = L_{j-1}x_{i,j-1} - L_j x_{i,j} + z_{i,j}^{\mathrm{L}}F_{i,j}^{\mathrm{L}} + N_{i,j}^{\mathrm{L}} + \sum_{k=1}^{r} v_{i,k}R_{k,j}\varepsilon_j^{\mathrm{L}} \tag{13}$$

where $N_{i,j}$ is the interfacial mass transfer rate.

The overall molar balances are obtained by summing Eqs. (12) and (13) over the total number of components $c$ in the mixture

$$\frac{\mathrm{d}M_j^{\mathrm{V}}}{\mathrm{d}t} = V_{j+1} - V_j + F_j^{\mathrm{V}} - \sum_{k=1}^{c} N_{k,j}^{\mathrm{V}} \tag{14}$$

$$\frac{\mathrm{d}M_j^{\mathrm{L}}}{\mathrm{d}t} = L_{j-1} - L_j + F_j^{\mathrm{L}} + \sum_{k=1}^{c} N_{i,j}^{\mathrm{L}} + \sum_{i=1}^{c}\sum_{k=1}^{r} v_{i,k}R_{k,j}\varepsilon_j^{\mathrm{L}} \tag{15}$$

The mole fractions of the vapor and liquid phases are calculated from the respective phase molar hold-ups:

$$y_{i,j} = \frac{M_{i,j}^{\mathrm{V}}}{M_j^{\mathrm{V}}}, \qquad x_{i,j} = \frac{M_{i,j}^{\mathrm{L}}}{M_j^{\mathrm{L}}} \tag{16}$$

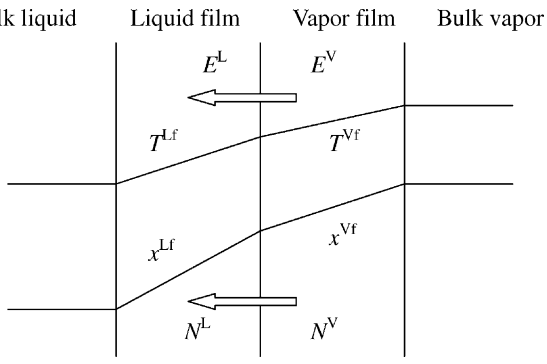


Fig. 4. Two-film model of the NEQ stage.

Table 3
Thermodynamic, physical properties and mass and energy transfer models used in the EQ and NEQ stage models

| | |
|---|---|
| *K*-value models | $k_i = \gamma_i P_i^0 / P$ |
| Equations of state | Virial equation |
| Molar volume | Data from [21,22] |
| Enthalpy | The modified Peng–Robinson (MPR) equation for the vapor enthalpy<br>The liquid phase enthalpy deduced from vapor phase enthalpy and evaporation heat |
| Activity coefficient | UNIFAC equation |
| Vapor pressure | Antoine equation |
| Viscosity | Orrick–Erbar equation for the liquid phase<br>Wilke equation for the vapor phase |
| Surface tension | Data from [21,22] |
| Thermal conductivity | Data from [21,22] |
| Binary mass transfer coefficient | AIChE method |
| Multi-component mass transfer coefficient | The generalized Maxwell–Stefan equation |
| Binary diffusion coefficient | Fuller–Schettler–Giddings equation for the vapor phase<br>Lusis–Ratcliff equation for the liquid phase at infinite dilution; Vignes method for the liquid phase at finite dilution [23] |
| Heat transfer coefficient | Calculated from the Chilton–Colburn *j*-factor [24] |

Only $c-1$ of these mole fractions are independent because the phase mole fractions sum to unity:

$$\sum_{k=1}^{c} y_{k,j} = 1, \qquad \sum_{k=1}^{c} x_{k,j} = 1 \tag{17}$$

The energy balance for the vapor and liquid phases are written as follows:

$$\frac{\mathrm{d}E_j^{\mathrm{V}}}{\mathrm{d}t} = V_{j+1}H_{j+1}^{\mathrm{V}} - V_j H_j^{\mathrm{V}} + F_j^{\mathrm{V}} H_j^{\mathrm{VF}} - E_j^{\mathrm{V}} - Q_j^{\mathrm{V}} \tag{18}$$

$$\frac{\mathrm{d}E_j^{\mathrm{L}}}{\mathrm{d}t} = L_{j-1}H_{j-1}^{\mathrm{L}} - L_j H_j^{\mathrm{L}} + F_j^{\mathrm{L}} H_j^{\mathrm{LF}} + E_j^{\mathrm{L}} - Q_j^{\mathrm{L}} \tag{19}$$

where $H_j^{\mathrm{V}}$ and $H_j^{\mathrm{L}}$ represent the molar enthalpy of vapor and liquid phases, respectively.

There is no need to take separate account in Eqs. (18) and (19) of the heat generated due to chemical reaction since the computed enthalpies include the heats of formation.

As has been said, the importance to model the NEQ is to set up the relation of interfacial mass and energy transfer rates. The molar transfer rate $N_i^{\mathrm{LF}}$ in the liquid phase is related to the chemical potential gradients by the Maxwell–Stefan equation:

$$\frac{x_i^{\mathrm{LF}}}{RT^{\mathrm{LF}}}\frac{\partial \mu_i^{\mathrm{LF}}}{\partial \eta} = \sum_{k=1}^{c} \frac{x_i^{\mathrm{LF}} N_k^{\mathrm{LF}} - x_k^{\mathrm{LF}} N_i^{\mathrm{LF}}}{C_t^{\mathrm{LF}} \kappa_{i,k}^{\mathrm{LF}} A} \tag{20}$$

$\kappa_{i,k}^{\mathrm{LF}}$ represents the mass transfer coefficient of the *i*–*k* pair in the liquid phase; this coefficient is estimated from information on the corresponding Maxwell–Stefan diffusivity $D_{i,k}^{\mathrm{L}}$ [20]. The summation equations at the interface are:

$$\sum_{k=1}^{c} y_{i,j}^{\mathrm{VF}} = 1, \qquad \sum_{k=1}^{c} x_{i,j}^{\mathrm{LF}} = 1 \tag{21}$$

The interphase energy transfer rates $E^{\mathrm{LF}}$ have conductive and convective contributions

$$E^{\mathrm{LF}} = -h^{\mathrm{LF}} A \frac{\partial T^{\mathrm{LF}}}{\partial \eta} + \sum_{i=1}^{c} N_i^{\mathrm{LF}} H_i^{\mathrm{LF}} \tag{22}$$

where $A$ is the interfacial area and $h^{\mathrm{LF}}$ is the heat transfer coefficient in the liquid phase. A relation analogous to Eq. (22) holds for the vapor phase.

At the vapor–liquid interface we assume phase equilibrium

$$y_{i,j}|_{\mathrm{I}} = K_{i,j} x_{i,j}|_{\mathrm{I}} \tag{23}$$

We also have continuity of mass and energy

$$N_i^{\mathrm{VF}}|_{\mathrm{I}} = N_i^{\mathrm{LF}}|_{\mathrm{I}}, \qquad E^{\mathrm{VF}}|_{\mathrm{I}} = E^{\mathrm{LF}}|_{\mathrm{I}} \tag{24}$$

Under steady-state conditions, all the time derivatives in the above equations are equal to zero. The combination of modified relaxation and Newton–Raphson methods where the equations are written in unsteady-state form and are integrated numerically until the steady-state solution has been found, is used to solve the above equations [16–19].

But both in the EQ stage model and in the NEQ stage model, the thermodynamic and physical properties are required. Moreover, in the NEQ stage model the mass and energy transfer models are also necessary. A list of the thermodynamic, physical properties and mass and energy transfer correlations available in our program [21–24] is provided in Table 3.

The simulation of the SCD column was performed on a PC (Pentium 4 1.5G). It took about 10 min for the EQ stage model and about 30 min for the NEQ stage model for a SCD column with 25 stages.

## 4. Comparison of experimental and simulation results

An experimental apparatus for producing C12 alkylbenzene shown in Fig. 5 was set up in laboratory. The SCD

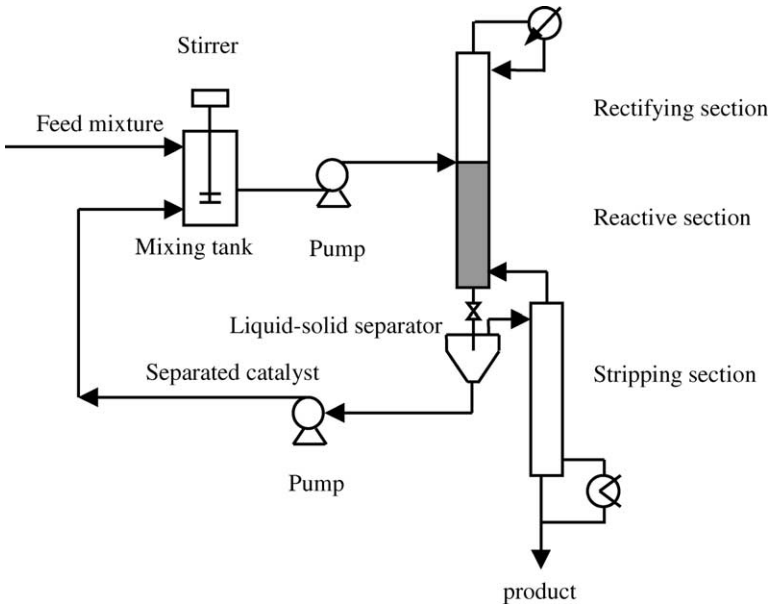


Fig. 5. Experimental flowsheet for producing C12 alkylbenzene.

column comprised of three parts, i.e. rectifying, reactive and stripping sections. The mixture of benzene, 1-dodecane and 1-dodecene was blend with catalyst in a mixing tank, and then into the top of the reactive section. 1-Dodecane was added to dilute the concentration of 1-dodecene and prevent it from polymerization. The catalyst was evenly distributed along the reactive section. The solid–liquid mixture leaving from the bottom of the reactive section was separated by a gas–liquid separator (high-speed shear dispersing machine). The resulting catalyst was sent to be regenerated and then recycled. The resulting liquid was the mixture of benzene, 1-dodecane, 1-dodecene and *i*-ph ($i$ = 2–6), which entered into the stripping section.

The SCD column had 23 trays and each was regarded as one model stage for both the EQ and NEQ stage models because the accurate prediction of tray efficiency was very difficult in the case of simultaneous multi-component separation and reaction. Therefore, the column was divided into 25 model stages in which the rectifying section had 5 stages, the reactive section 10 stages and the stripping section 8 stages. The reboiler was stage 1 and the total condenser stage 25. Some structural and operating parameters are listed in Table 4. In the experiment, the column pressure was adjustable, at 101.3, 131.7 and 162.1 kPa, respectively, while other operating parameters remained constant.

In the simulation of the EQ and NEQ stage models, for simplifying the computer program, *i*-ph ($i$ = 2–6) were taken on as one component because they had similar thermodynamic and physical properties.

Figs. 6–8 show the temperature profiles along the SCD column at pressures 101.3, 131.7 and 162.1 kPa, respectively. It can be seen that the calculated values by the NEQ stage model are much closer to the experimental values than by the EQ stage model. The reason may be that in actual operation, trays rarely, if ever, operate at equilibrium. We know that for conventional distillation operation with vapor–liquid two phases, the tray efficiency cannot reach 100% in most cases. However, in the reactive section of the SCD column there are vapor–liquid–solid three phases. The addition of solid particles will decrease the tray efficiency in this case because the presence of solid particles close to the interface may hold back the mass transfer of vapor and liquid phases and reduce the contact area of two phases [25,26]. So the prediction of the EQ stage model is not accurate in the case of multi-component separation and chemical reaction with vapor–liquid–solid three phases. It is the rate of mass and heat transfer, and not the equilibrium that often limits the separation.

Table 4
The structural and operating parameters of the SCD column

| Structural parameters | | Operating parameters | |
|---|---|---|---|
| Type of tray | Sieve | Pressure (kPa) | 101.3, 131.7, 162.1 |
| Column diameter (m) | 0.05 | Reflux rate ($g\,h^{-1}$) | 700 |
| Total tray area ($m^2$) | 0.002 | Feed rate ($g\,h^{-1}$) | |
| Number of liquid flow passes | 1 | Benzene | 35 |
| Tray spacing (m) | 0.1 | 1-Dodecene | 50.4 |
| Liquid flow path length (m) | 0.04 | 1-Dodecane | 749.6 |
| Active area ($m^2$) | 0.002 | The concentration of catalyst in the feed mixture ($g\,ml^{-1}$) | 0.05 |
| Downcomer type | Round | | |
| Downcomer clearance (m) | 0.04 | | |
| Weir length (m) | 0.03 | | |
| Weir height (m) | 0.03 | | |

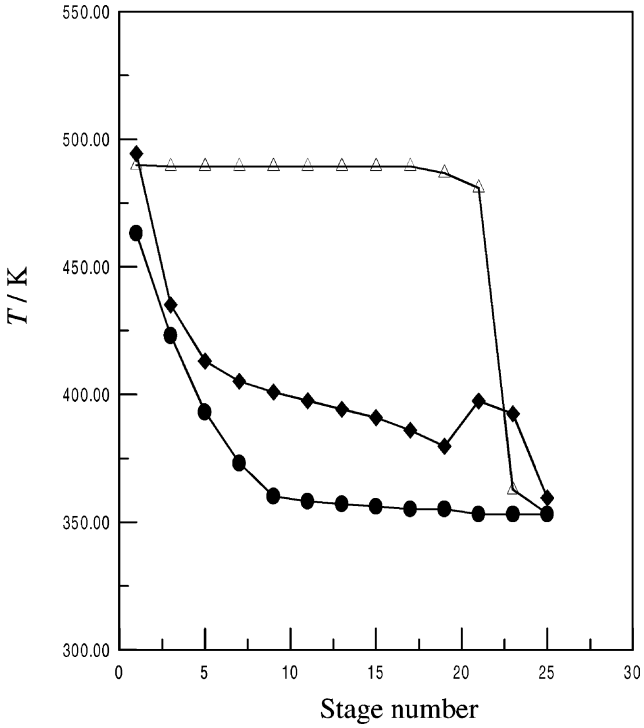


Fig. 6. Comparison of calculated and experimental values at 101.3 kPa. The tray is numbered from the bottom to the top: (●) experimental values; (◆) calculated values by the NEQ stage model; (△) calculated values by the EQ stage model.

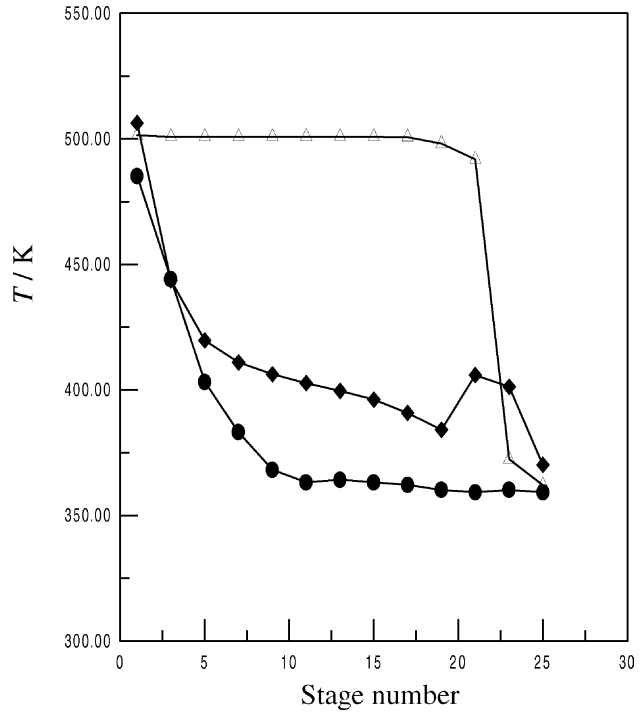


Fig. 7. Comparison of calculated and experimental values at 131.7 kPa. The tray is numbered from the bottom to the top: (●) experimental values; (◆) calculated values by the NEQ stage model; (△) calculated values by the EQ stage model.

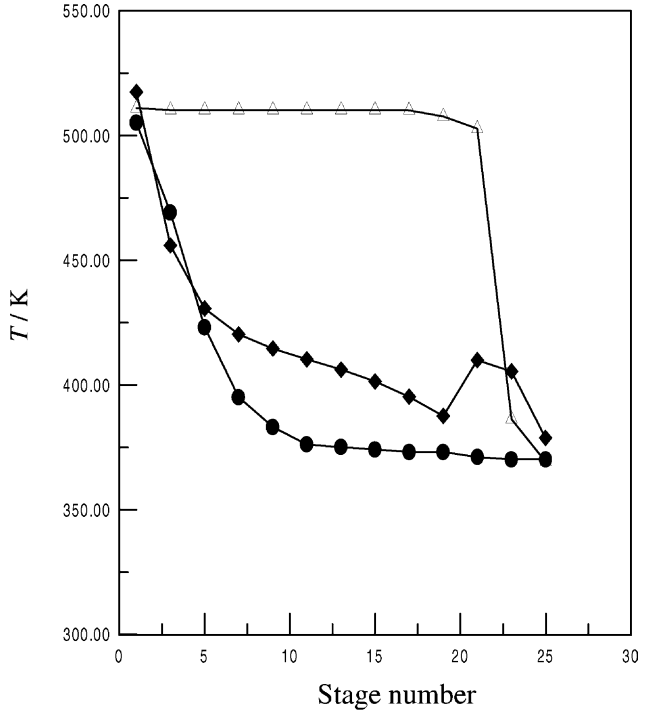


Fig. 8. Comparison of calculated and experimental values at 162.1 kPa. The tray is numbered from the bottom to the top: (●) experimental values; (◆) calculated values by the NEQ stage model; (△) calculated values by the EQ stage model.

The difference of calculated values between the EQ and NEQ models can also be brought out in the composition profiles along the column, which are illustrated in Figs. 9 and 10. In this work, the studied system is special and the boiling-point difference of the key light (benzene) and heavy (1-dodecene) components is very high, up to 133.2 °C. This means that these two components are easy to be separated in the equilibrium stages. So there is an abrupt change of benzene composition in the feed tray in Fig. 9 for the EQ stage model. In the reactive and stripping sections of the SCD column, the benzene composition is nearly zero, which leads to the higher temperature and fewer product of *i*-ph ($i$ = 2–6) than actual operation. However, the change of benzene composition in the feed tray in Fig. 10 for the NEQ stage model is somewhat smooth. In many places of the reactive and stripping sections for the NEQ stage model, the benzene composition is away from zero, which leads to the lower temperature and more products of *i*-ph ($i$ = 2–6) than for the EQ stage model. Therefore, the calculated values by the NEQ stage model are more in agreement with the experimental values.

Because the deviation between the experimental and calculated values is large for the EQ stage model, the tray efficiency under the operation condition shown in Table 4 is low. That is to say, the assumption of EQ stage is far away from the fact. But for the NEQ stage model there is a little fluctuation of temperatures in the vicinity of the feed tray, which may be due to the great influence of the feed mixture

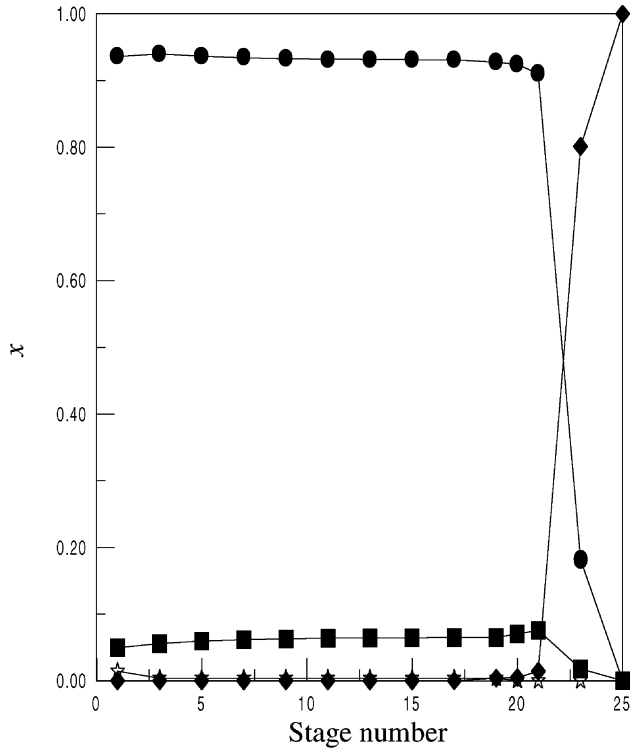


Fig. 9. Composition profile of the SCD column for the EQ stage model. The tray is numbered from the bottom to the top: (◆) benzene; (■) 1-dodecene; (●) 1-dodecane; (☆) *i*-ph.

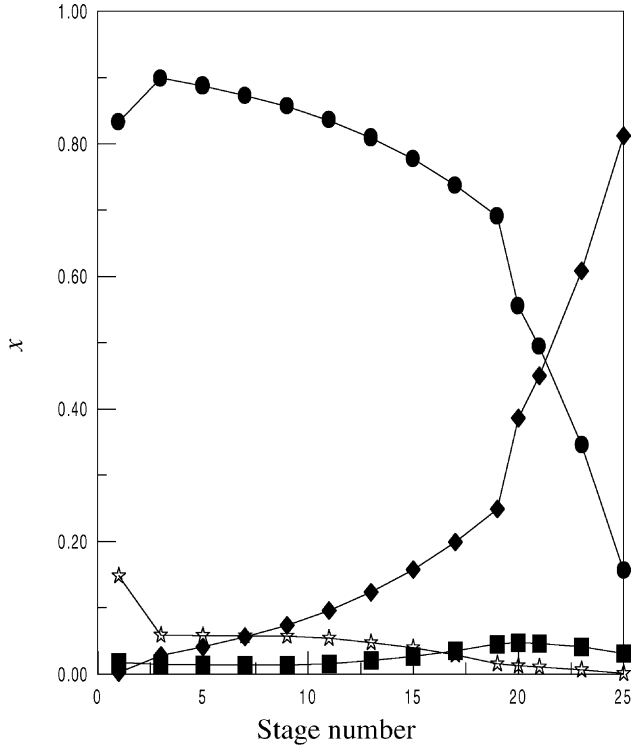


Fig. 10. Composition profile of the SCD column for the NEQ stage model. The tray is numbered from the bottom to the top: (◆) benzene; (■) 1-dodecene; (●) 1-dodecane; (☆) *i*-ph.

Table 5
The product composition at the bottom of the SCD column at pressure 101.3 kPa

| | $x^{exp}$ | $x^{cal}$ | |
|---|---|---|---|
| | | EQ stage model | NEQ stage model |
| Benzene | 0.0 | 0.0 | 0.0036 |
| 1-Dodecene | 0.0 | 0.0497 | 0.0113 |
| 1-Dodecane | 0.8926 | 0.9361 | 0.8850 |
| C12 alkylbenzene | 0.1074 | 0.0142 | 0.1001 |

on the mass and heat transfer rates and the limitation of accuracy of thermodynamic equations used in the NEQ stage model.

A comparison of the product composition at the bottom between the experimental and calculated values is also made in Table 5 where $x$ is the mole fraction in the liquid phase. Table 5 shows that the concentrations of both benzene and 1-dodecene at the bottom are very low, which proves that the SCD column is effective for this alkylation reaction. Furthermore, it can be seen from Table 5 that the calculated values by the NEQ stage model are more approximate to the experimental values than by the EQ stage model. So it further proves that the NEQ model is reliable and can be used for the design and optimization of the SCD column.

The NEQ stage model should be preferred for the simulation of a tray column for reactive distillation to the EQ stage model. However, as pointed out by Lee and Dudukovic [10], a close agreement between the predictions of EQ and NEQ models can be found if the tray efficiency is accurately predicted for the EQ model. But in most cases the tray efficiency is difficult to predict, especially for the vapor–liquid–solid three phases system.

In the experiment, the conversion of 1-dodecene 100% and selectivity of 1-dodecene 100% are obtained. Moreover, the weight concentration of 2-ph in the *i*-ph is up to 35%, which is higher than 25% reported in the fixed-bed reactor [2]. So the SCD column is positive to the selectivity of 2-ph, which is favorable in the industry.

## 5. Conclusion

Due to the unique advantages of the SCD column, it is very straightforward to combine this technology with the synthesis of C12 alkylbenzene with benzene and 1-dodecene. Since C12 alkylbenzene is widely used as raw materials for detergents, alkylation of benzene and 1-dodecene has a lasting value in the industry. In this work, silica gel supported by tungstophosphoric acid (HPW) is used as catalyst. The kinetic equations over this catalyst are obtained in a fixed-bed laboratory micro-reactor. On this basis, the EQ and NEQ stage models have been established to simulate the SCD column. An experimental apparatus for producing C12 alkylbenzene in the SCD column has also been set up, and the experimental results prove that the SCD

column is effective for the alkylation reaction. Moreover, the comparison of experimental and calculated values is also made, and it is concluded that the NEQ stage model is more accurate than the EQ stage model. The reason may be that in actual operation, trays rarely, if ever, operate at equilibrium, especially when the solid particles are added in the SCD column. So it is advisable to select the NEQ stage model for the design and optimization of the SCD column, which helps the future scale-up of the SCD techniques in the industry.

## Acknowledgements

This work is supported by the State Key Basic Research Program (No. G2000048006).

## References

[1] J.L.G. Almeida, M. Dufaux, Y.B. Taarit, Linear alkylation, JAOCS 71 (7) (1994) 675–694.
[2] B. Vora, P. Pujado, I. Imai, Production of detergent olefins and linear alkylation, Chem. Eng. 19 (1990) 187–191.
[3] L.Y. Wen, E. Min, Development of solid heteropoly acid catalyst, Petrochem. Technol. (China) 29 (2000) 49–55.
[4] Y.X. Zhang, X. Xu, Study on catalytic distillation process. Part II. Simulation of catalytic distillation processes, Trans. IChemE 70 (1992) 465–470.
[5] L.A. Smith, M.N. Huddleston, New MTBE design now commercial, Hydrocarbon Process. March (1982) 121–123.
[6] H.S. Subawalla, J.R. Fair, Design guidelines for solid-catalyzed reactive distillation systems, Ind. Eng. Chem. Res. 38 (1999) 3696–3709.
[7] A.V. Solokhin, S.A. Blagov, Reactive distillation is an advanced technique of reaction process operation, Chem. Eng. Sci. 51 (1996) 2559–2564.
[8] L.Y. Wen, E. Min, G.C. Pang, Synthesis of cumene by suspension catalytic distillation process, J. Chem. Ind. Eng. (China) 51 (2000) 115–119.
[9] J.D. Shoemaker, E.M. Jones, Cumene by catalytic distillation, Hydrocarbon Process. June (1987) 57–58.
[10] J.H. Lee, M.P. Dudukovic, A comparison of the equilibrium and nonequilibrium models for a multicomponent reactive distillation column, Comput. Chem. Eng. 23 (1998) 159–172.
[11] R. Taylor, R. Krishna, Modelling reactive distillation, Chem. Eng. Sci. 55 (2000) 5183–5229.
[12] R. Baur, A.P. Higler, R. Taylor, R. Krishna, Comparison of equilibrium stage and nonequilibrium stage models for reactive distillation, Chem. Eng. J. 76 (2000) 33–47.
[13] R. Baur, R. Taylor, R. Krishna, Dynamic behaviour of reactive distillation columns described by a nonequilibrium stage model, Chem. Eng. Sci. 56 (2001) 2085–2102.
[14] A.P. Higler, R. Taylor, R. Krishna, The influence of mass transfer and mixing on the performance of a tray column for reactive distillation, Chem. Eng. Sci. 54 (1999) 2873–2881.
[15] A.P. Higler, R. Taylor, R. Krishna, Nonequilibrium modeling of reactive distillation: multiple steady states in MTBE synthesis, Chem. Eng. Sci. 54 (1999) 1389–1395.
[16] H. Komatsu, Application of the relaxation method of solving reacting distillation problems, J. Chem. Eng. Japan 10 (1977) 200–205.
[17] H. Komatsu, C.D. Holland, A new method of convergence for solving reacting distillation problems, J. Chem. Eng. Japan 10 (1977) 292–297.
[18] J. Jelinek, V. Hlavacek, Steady state countercurrent equilibrium stage separation with chemical reaction by relaxation method, Chem. Eng. Commun. 2 (1976) 79–85.
[19] R. Taylor, H.A. Kooijman, J.S. Hung, A second generation nonequilibrium model for computer simulation of multicomponent separation process, Comput. Chem. Eng. 18 (1994) 205–217.
[20] R. Krishna, J.A. Wesselingh, The Maxwell–Stefan approach to mass transfer, Chem. Eng. Sci. 52 (1997) 861–911.
[21] J.S. Tong, The Fluid Thermodynamics Properties, Petroleum Technology Press, Beijing, 1996.
[22] R.C. Reid, J.M. Prausnitz, T.K. Sherwood, The Properties of Gases and Liquids, McGraw-Hill, New York, 1987.
[23] H.A. Kooijman, R. Taylor, Estimation of diffusion coefficients in multicomponent liquid systems, Ind. Eng. Chem. Res. 30 (1991) 1217–1222.
[24] J.D. Seader, E.J. Henley, Separation Process Principles, Wiley, New York, 1998.
[25] E. Alper, B. Wichtendahl, W.D. Deckwer, Gas absorption mechanism in catalytic slurry reactions, Chem. Eng. Sci. 35 (1980) 217–222.
[26] A.A.C.M. Beenackers, W.P.M.V. Swaaaij, Mass transfer in gas–liquid slurry reactors, Chem. Eng. Sci. 48 (1993) 3109–3139.